metals

MDPI

Article

Arsenate and Arsenite Sorption Using Biogenic Iron Compounds: Treatment of Real Polluted Waters in Batch and Continuous Systems

Laura Castro [1,2,*], Lesly Antonieta Ayala [2], Arevik Vardanyan [3], Ruiyong Zhang [4,5] and Jesús Ángel Muñoz [2]

1 Department of Applied Mathematics, Materials Science and Engineering and Electronic Technology, School of Experimental Sciences and Technology, Rey Juan Carlos University, 28935 Móstoles, Spain
2 Department of Chemical and Materials Engineering, University Complutense of Madrid, 28040 Madrid, Spain; leslyaay@ucm.es (L.A.A.); jamunoz@ucm.es (J.Á.M.)
3 Department of Microbiology, SPC "Armbiotechnology" of the National Academy of Sciences of Armenia, Yerevan 0056, Armenia; arevik.vardanyan@asnet.am
4 Key Laboratory of Marine Environmental Corrosion and Biofouling, Institute of Oceanology, Chinese Academy of Sciences, Qingdao 266071, China; ruiyong.zhang@qdio.ac.cn
5 Open Studio for Marine Corrosion and Protection, Pilot National Laboratory for Marine Science and Technology (Qingdao), Qingdao 266237, China
* Correspondence: laura.castro@urjc.es

Abstract: Arsenic pollution in waters is due to natural and anthropogenic sources. Human exposure to arsenic is associated with acute health problems in areas with high concentrations of this element. Nanometric iron compounds with large specific surface areas and higher binding energy produced by some anaerobic microorganisms are thus expected to be more efficient adsorbents for the removal of harmful metals and metalloids than chemically produced iron oxides. In this study, a natural consortium from an abandoned mine site containing mainly *Clostridium* species was used to biosynthesize solid Fe(II) compounds, siderite ($FeCO_3$) and iron oxides. Biogenic precipitates were used as adsorbents in contact with solutions containing arsenate and arsenite. The adsorption of As(V) fitted to the Langmuir model (q_{max} = 0.64 mmol/g, K_L = 0.019 mmol/L) at the optimal pH value (pH 2), while the As(III) adsorption mechanism was better represented by the Freundlich model (K_F = 0.476 L/g, n = 2.13) at pH 10. Water samples from the Caracarani River (Chile) with high contents of arsenic and zinc were treated with a biogenic precipitate encapsulated in alginate beads in continuous systems. The optimal operation conditions were low feed flow rate and the up-flow system, which significantly improved the contaminant uptake. This study demonstrates the feasibility of the application of biogenic iron compounds in the treatment of polluted waters.

Keywords: arsenic; biogenic iron compounds; adsorption; alginate beads; water treatment

Citation: Castro, L.; Ayala, L.A.; Vardanyan, A.; Zhang, R.; Muñoz, J.Á. Arsenate and Arsenite Sorption Using Biogenic Iron Compounds: Treatment of Real Polluted Waters in Batch and Continuous Systems. *Metals* **2021**, *11*, 1608. https://doi.org/10.3390/met11101608

Academic Editor: Antoni Roca

Received: 31 August 2021
Accepted: 8 October 2021
Published: 10 October 2021

1. Introduction

Arsenic is one of the most toxic elements and its incorporation into the environment results from natural weathering and anthropogenic activities. Arsenic exists in several oxidation states; however, the predominant species in aqueous solution are As(III) and As(V), which are considered a major environmental problem. Exposure to arsenic mainly occurs through drinking water and causes several health risks in the human body including cancer, skin damage and circulatory problems [1]. Arsenic is highly toxic even at trace-level concentrations and enters the food chain mainly from contaminated water [2]; in consequence, regulations are enforced to reduce the admissible levels of arsenic in water [3].

Conventional water treatment methods such as precipitation, filtration, flotation, ion exchange or reverse osmosis are complex, energy-intensive and costly. Membranes have been demonstrated to be an effective method that removes not only arsenic, but other water contaminants. Nanofiltration and reverse osmosis present a high removal

efficiency (>99%). Nevertheless, nanofiltration can overtake reverse osmosis in terms of higher flux for the same rate of removal of arsenic while permitting filtration at a lower pressure than is necessary for reverse osmosis [4]. Physicochemical separation through chemical coagulation and precipitation can treat water in large volumes, but the degree of purification is low (90–92%) compared to membrane separation. Disposal of a great amount of sludge is also problem. Oxidants such as ozone, hydrogen peroxide, chlorine, and permanganate in arsenic removal processes are used mainly for changing oxidation states of As(III) to As(V) [5].

Adsorption has arisen as a feasible alternative for the metal and metalloid removal from polluted waters. Activated carbon-based adsorbents have been produced using any natural materials with high carbon content. Activated carbon is a cost-effective and efficient adsorbent because it is a microporous non-graphite form of carbon with a high internal porosity. It was observed that As(V) is better adsorbed than As(III) [6].

Furthermore, a very large number of metal-based adsorbents have been developed for arsenic removal over the years, such as iron oxide coated sand, activated alumina, MnO_2, TiO_2 and zeolites. Nanomaterials present special physicochemical properties offering a high specific surface compared to traditional adsorbents and, consequently, reaching faster uptake kinetics [7]. Iron oxides are efficient for the removal of metals, such as uranium, molybdenum and chromium by adsorption, and also for the chemical reduction of nitroaromatics and dechlorinated aliphatics [8,9]. The biosynthesis of nanoparticles is an environmentally friendly alternative to traditional methods to produce nanometric adsorbents and many microorganisms can use iron for a variety of purposes and are involved in its biogeochemical cycle [10]. Most of the research developed on adsorption/biosorption is still at the stage of laboratory studies [11]. Previous works scarcely report the treatment of potentially toxic metals from industrial effluents using natural materials in continuous systems and have limited industrial application because several metal and metalloid ions and other contaminants are present in wastewaters [12,13].

Acidithiobacillus ferrooxidans precipitates iron schwertmannite and the regulation of the pH modifies the precipitation efficiency and the specific surface area of the biogenic mineral. This effect has an impact on the removal of arsenic, increasing the uptake rate from 52.9% to 92.7–97.8% due to the formation of mesopores [14].

Bacterial sulfate reduction is able to produce biogenic pyrite nanoparticles, which remove arsenic from groundwaters by adsorption and co-precipitation from its initial concentration of 0.3–0.5 mg/L to below the legal standards (0.05 mg/L) [15].

Nano-sized FeS-coated limestone biosynthesized by iron-reducing bacterium *Acidiphilium cryptum* JF-5 and a sulfate-reducing bacterium was used to remove As(V) from the solution. FeS coated limestone significantly improved the adsorption efficiency of As(V) in comparison to limestone alone from 6.64 μg/g to 187 μg/g in both batch and column experiments [16].

Fe-sericite composite beads presented a high adsorption of As(V) and phosphate (5.780 and 4.446 mg/g for As(V) and phosphate, respectively) within a wide range of pH values. Furthermore, Fe-sericite composite beads in a fixed-bed column were able to adsorb As(V) and phosphate, also under dynamic conditions [17].

The objective of this work was to study the adsorption of arsenic oxyanions using nanometric iron precipitates generated by a natural microbial consortium. The biogenic iron compounds were used as adsorbents in solutions containing arsenate and arsenite to investigate the characteristics of the adsorption process: effect of the pH value and initial concentration in solution, adsorption isotherms and kinetics. Water from the Caracarani River (Chile) polluted with a high concentration of arsenic was put in contact with the biogenic precipitates to remove the contaminants. Furthermore, continuous experiments were carried out with columns under different conditions: real and synthetic solutions, different feed flow rate, different height of fixed bed and direct and reverse feed flow.

2. Materials and Methods

2.1. Adsorbents

An iron-reducing microbial consortium from an abandoned mine near La Unión (Murcia, Spain) precipitated iron compounds using soluble ferric citrate as the iron source. These biogenic precipitates were identified as siderite ($FeCO_3$), magnetite (Fe_3O_4) and vivianite ($Fe_3(PO_4)_2 \cdot 8H_2O$). The surface area of the biogenic iron compounds was 56.98 m^2/g. The pore volume was 0.122 cm^3/g and the average pore size 83 Å [18].

To obtain alginate beads encapsulating the biogenic iron compounds, 20 g/L of the air-dried precipitates were dispersed in an aqueous solution of sodium alginate in a concentration of 20 g/L. The dispersion was pressed through a syringe (internal diameter of 0.5 mm) and dropped into 3% $CaCl_2$ solution.

The adsorbents used in the experiments (biogenic iron precipitates and beads) were observed in a scanning electron microscope (SEM) (JEOL JSM-6330 F, Yamagata, Japan). Before the observation, the samples were coated with a thin layer of gold.

2.2. Batch Experiments

The adsorption experiments were performed with synthetic solutions prepared with sodium arsenite ($NaAsO_2$) and hydrated sodium arsenate ($Na_2HAsO_4 \cdot 7H_2O$) provided by Fisher Scientific (Loughborough, UK). The initial pH of solutions was adjusted with diluted H_2SO_4 and with NaOH. The biogenic iron compounds were placed in contact with solutions in glass Erlenmeyers stirred at a rotation speed of 150 rpm and at room temperature (25 ± 1 °C). Liquid samples were collected at different times (0, 15, 30, 60 and 120 min) and metalloid concentrations were measured by ICP-OES (Perkin Elmer Optima 2100 DV, Wellesley, MA, USA) (plasma gas (Ar) flow rate: 15 L/min; pumping rate: 1.50 mL/min). Kinetic studies were performed at different initial pH values (2, 4, 7 and 10) adding 1 g/L of iron precipitates to continuously stirred flasks containing 100 mL of 50 mg/L As(III) or As(V) solutions. Adsorption isotherms were also performed at the optimal pH value and at constant temperature by varying the initial arsenic concentration from 10 to 100 mg/L.

The biogenic adsorbents were also used for the treatment of polluted water from the Caracarani River (upper Lluta River basin, Chile). The Azufre River and the Caracarani River confluence and from this point downstream is also named Caracarani River. The Azufre River ("sulfur river" in English) has its source at the Tacora volcano, near an abandoned sulfur mine and tailings site. The oxidation of sulfur tailings and volcanic geothermal springs generate an acidic stream (pH < 2) containing several potentially toxic elements. In contrast, the Caracarani River presents a pH value between 8.2 and 8.6 [19,20]. The main characteristics of the water used in the experiments are shown in Table 1.

Table 1. Characterization of the Caracarani River waters used in the adsorption tests.

pH	Redox Potential	Conductivity (mS/cm)	Fe (mg/L)	As (mg/L)	Zn (mg/L)
2.24	706	4.84	127 ± 18	3.2 ± 0.1	10 ± 5

Adsorption experiments with Caracarani River water were performed by adding 1 g/L of adsorbent (biogenic precipitates or precipitates encapsulated in alginate beads) to Erlenmeyer flasks containing 100 mL of dissolution under stirring at room temperature. Sampling was performed periodically, and zinc and arsenic concentrations were determined by ICP-OES (Perkin Elmer Optima 2100 DV, Wellesley, MA, USA).

All the adsorption tests were performed in duplicates, and the average measurements were used for data processing.

2.3. Continuous Sorption Tests

Continuous adsorption experiments were performed with polluted water from Caracarani River using small glass columns (2.5 cm inner diameter and 15 cm length) packed with

biogenic iron precipitates encapsulated in alginate beads (~14% hollow volume). The initial pH value of the solution was 2.2 (pH of the samples as received). That pH gave the highest uptakes in previous batch experiments carried out with these adsorbents, and the metal precipitation is avoided at this pH value. The polluted water was introduced to the columns using a peristaltic pump (MasterFlex L/S, Vernon Hills, IL, USA). In order to ensure a good distribution of solution and to prevent the loss of adsorbent, glass wool was placed on the top and bottom of the column.

2.4. Characterization Techniques

Iron precipitates produced by the natural microbial consortium and the alginate beads encapsulating the biogenic precipitates were coated with a thin layer of gold and observed using a scanning electron microscope (SEM) (JEOL JSM-6330 F, Yamagata, Japan).

Microbially precipitated iron compounds were analyzed after the adsorption experiments using powder X-ray diffraction (XRD) on a Philips X′pert-MPD (Malvern Panalytical, Malvern, UK) with a Cu anode operating at a wavelength of 1.5406 Å as the X-ray source.

3. Results

3.1. Batch Experiments

3.1.1. Effect of pH

The adsorbent generated by this microbial consortium from an abandoned mining area showed its ability to remove several hazardous species in a previous study, especially chromate and arsenate [18]. The solution pH influences both the adsorbent and the chemistry of the metals and metalloids in solution. In this work, the experiments were performed with an initial arsenic concentration of 50 mg/L and adsorption time of 2 h. The pH range of the study was 2 to 10 for arsenite and arsenate, which are soluble at any pH (Figure 1).

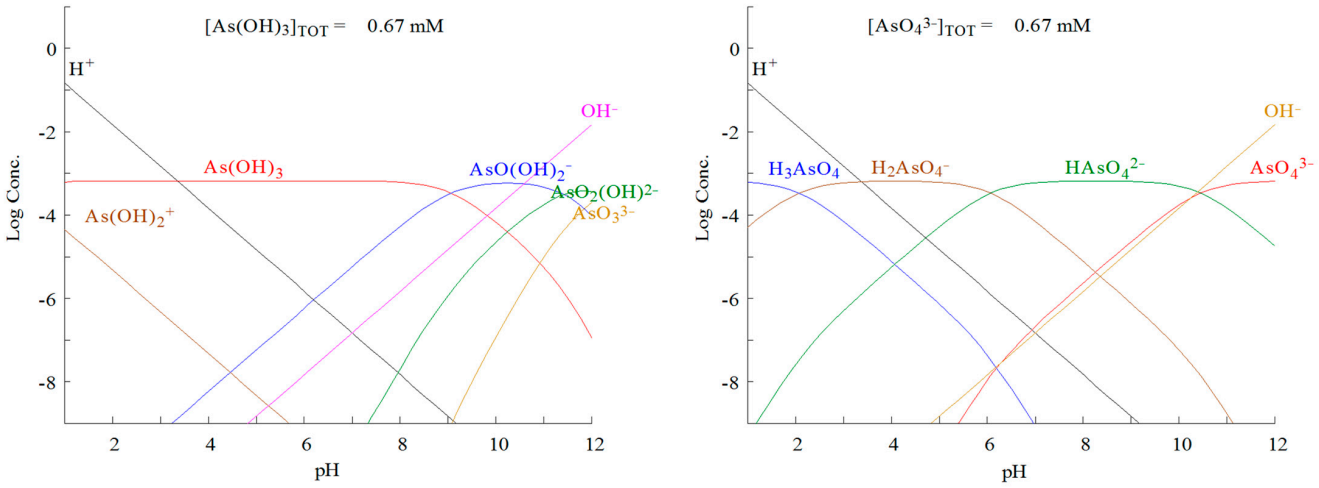

Figure 1. Speciation diagrams for As(III) and As(V) as a function of pH for a total arsenic concentration of 50 mg/L obtained using Hydra and Medusa software (KTH Royal Institute of Technology, Stockholm, Sweden).

Figure 2 shows the As(III) and As(V) adsorption using the iron compounds biosynthesized by the natural consortium at different initial pH values. The adsorption of oxyanions on iron precipitates is strongly influenced by the pH value of the solution. The pH modifies the chemistry of the metalloids and the binding sites due to the protonation of functional groups. Arsenate adsorption was higher at an acidic pH because the surface of the iron compounds has a net positive charge that would attract oxyanions. Conversely, arsenite was better adsorbed at higher pH values because its deprotonation takes place over pH 8. This behavior is caused by the electrostatic interaction between the arsenic oxyanions and the surface of the biogenic iron compounds with positive charge [18].

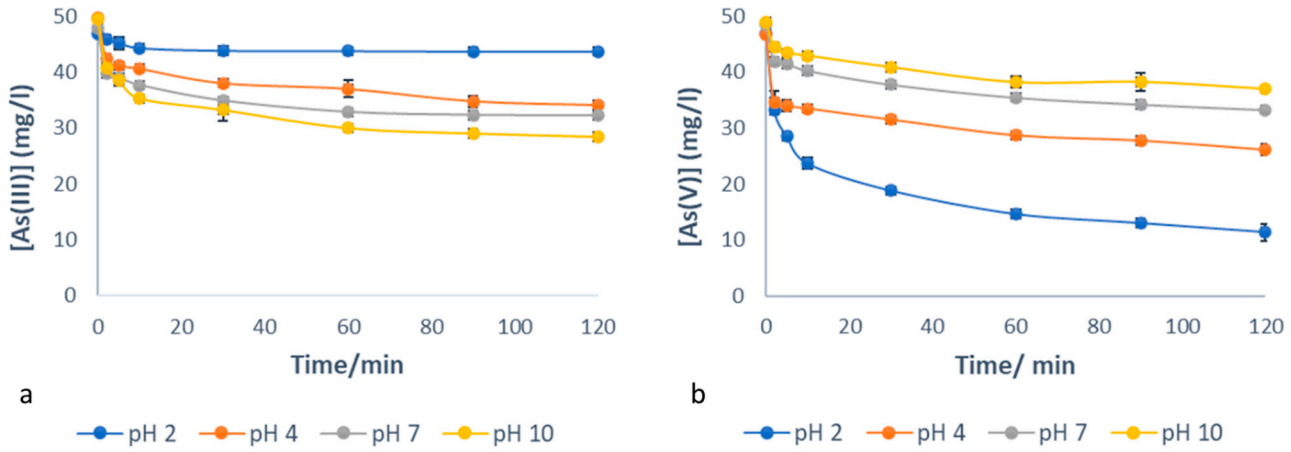

Figure 2. Effect of pH value on arsenic adsorption by biogenic iron precipitates (1 g/L of adsorbent) from (**a**) arsenite solutions (C_0 (As(III)) = 50 mg/L) and (**b**) arsenate solutions (C_0 (As(V)) = 50 mg/L).

3.1.2. Effect of Arsenic Concentration

Arsenic concentration is also a relevant variable during the adsorption onto biogenic iron precipitates. Electrostatic interactions between functional groups and toxic ions have a significant effect on the nexus between initial concentration and metalloid uptake. Kinetic studies were carried out at different arsenic concentrations to determine adsorption parameters using models (Figure 3).

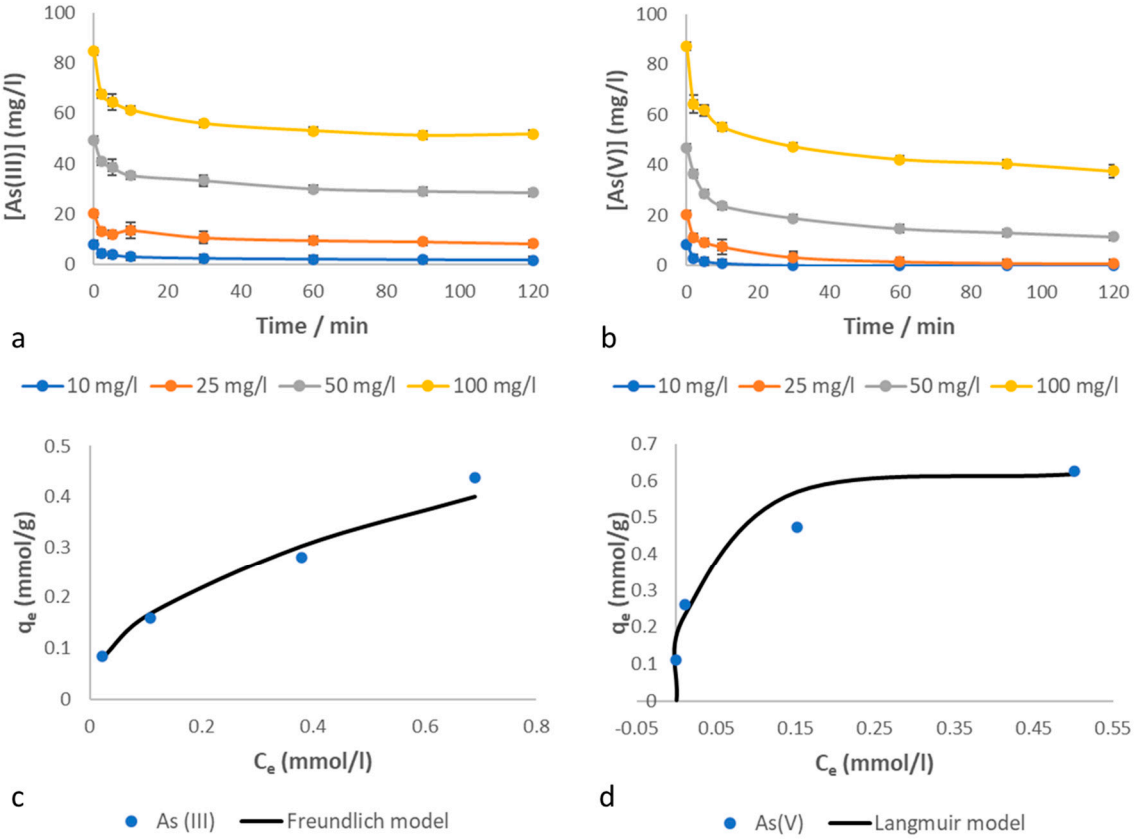

Figure 3. Effect of arsenic concentration on adsorption by biogenic iron precipitates (1 g/L of adsorbent) from (**a**) arsenite solutions at pH 10 and (**b**) arsenate solutions at pH 2. Experimental data and predicted adsorption isotherms: (**c**) As(III) fitted to Freundlich model and (**d**) As (V) fitted to non-linear Langmuir model.

Metalloid adsorption occurs in three steps. Firstly, the adsorbate in the solution is transferred to the external surface of the adsorbent, then the adsorbate diffuses internally to the binding sites and finally the adsorption takes place itself. The adsorption step is considered the slowest step in the different models.

The uptake mechanisms are determined by the isotherms and their characteristic parameters (adsorbent capacities and affinity) are specific for each system. Data obtained in adsorption experiments for arsenate and arsenite onto the biogenic iron precipitates were fitted to the Langmuir and Freundlich models.

The Langmuir model is applied to monolayer adsorption where the adsorbate is bound at homogeneous active sites on the adsorbent surface, and adsorption is independent of the number of occupied sites. A Langmuir isotherm can be expressed by the following equation:

$$q = \frac{q_{max} \cdot C_e}{K_L + C_e} \quad (1)$$

where q is the adsorption capacity and C_e is the metalloid concentration.

The Freundlich model is an empirical model, which assumes multilayer adsorption with interaction between molecules on the adsorbent surface. The mathematical expression for this model is

$$q = K_F \cdot C_e^{\frac{1}{n}} \quad (2)$$

where K_F is a constant related to the adsorption capacity and n (dimensionless) is a constant that indicates the nature and the effectiveness of the adsorption.

The adsorption mechanism and isotherm model can be different for a given adsorbent if there are different species in solution. C_e/q was graphically represented versus C_e to obtain a linear regression to directly calculate the Langmuir parameters, q_{max} and b (inverse of K_L) values. Furthermore, log q_e was plotted versus log C_e and the linear regression analysis was used to determine n and K_F (Table 2).

The adsorption of As(V) onto biogenic precipitates fitted better to the Langmuir model, while the As(III) adsorption mechanism was better represented by the Freundlich model. In the Langmuir model, the effectiveness of the adsorbent is greater when the q_{max} and K_L values are lower. In the Freundlich model, a higher value of K_F indicates a higher adsorption capacity and higher values of n reflect a diminishing tendency for sorption with increasing uptake. Despite of the experimental results with different arsenic species fitted to different models, the arsenate adsorption seemed to be more effective than arsenite removal.

Table 2. Langmuir and Freundlich parameters for As(III) and As(V) adsorption isotherms on the iron precipitates generated by the microbial consortium.

Adsorbate	pH	Langmuir Parameters			Freundlich Parameters		
		q_{max} (mmol/g)	K_L (mmol/L)	R^2	K_F (L/g)	n	R^2
As(III)	10	0.52	0.21	0.90	0.476	2.13	0.98
As(V)	2	0.64	0.019	0.99	0.636	6.25	0.91

A comparison between the maximum adsorption capacities of the biogenic iron precipitates and other iron-based adsorbents under similar conditions is shown in Table 3. Different adsorbents have been tested for arsenic removal due to the high effectiveness of iron compounds for adsorption. Nevertheless, great differences are observed in their adsorption capacities mainly related to their particle size. Nanostructures exhibited the highest capacities. The micro-/nanostructructures precipitated by the microbial consortium presented good properties as arsenic adsorbents compared to other tested materials.

Table 3. Comparison of maximum arsenic adsorption capacities of biogenic iron precipitates with other iron-based adsorbents.

Adsorbent	Adsorbate	q_c (mg/g)	Reference
Fe(III)-natural zeolitic tuff	As(V)	1.55	[21]
Graphene oxide iron nanohybrid	As(III)	306	[22]
	As(V)	431	
Fe-attapulgite	As (V)	5.2	[23]
Nanostructured hollow iron-cerium alkoxides	As(III)	266.0	[24]
	As(V)	206.6	
Iron-coated seaweed	As(III)	4.2	[25]
	As(V)	7.3	
Iron-oxide-coated sponge	As(III)	4.2	[26]
	As(V)	4.6	
Core-shell magnetic composite	As(V)	13.47	[27]
Biogenic iron precipitates	As(III)	38.96	This study
	As(V)	47.95	

The microbial consortium generated a precipitate under anaerobic conditions containing Fe(II): siderite ($FeCO_3$), magnetite (Fe_3O_4) and vivianite ($Fe_3(PO_4)_2{\cdot}8H_2O$). The residues were also analyzed by X-ray diffraction after the adsorption experiments with As(III) and As(V) in solution (Figure 4).

Both As(III) and As(V) are strongly adsorbed onto the iron precipitate surface through surface complexation and surface precipitation processes. These processes depend on the arsenic oxidation state [28]. It has been reported that As(III) binds to iron-bearing minerals by tridentate complexation in a first stage. Then, As(III) and As(V) form amorphous and nanocrystalline surface precipitates [29,30]. Figure 4a reveals the occurrence of As(III) precipitates with low crystallinity, As_4O_6 and As_2O_3. In contrast, the few works that have reported the interaction of As(V) with Fe(II)-bearing minerals suggest that adsorption and precipitation processes leads to different arsenic speciation [31]. The initial adsorbed As(V) is partially reduced, most probably due to the presence of Fe(II) in the biogenic iron compound produced under anaerobic conditions. As shown in Figure 4b, the complexation and reduction of As(V) occurred, and the final products were As_2O and As that covered the adsorbent.

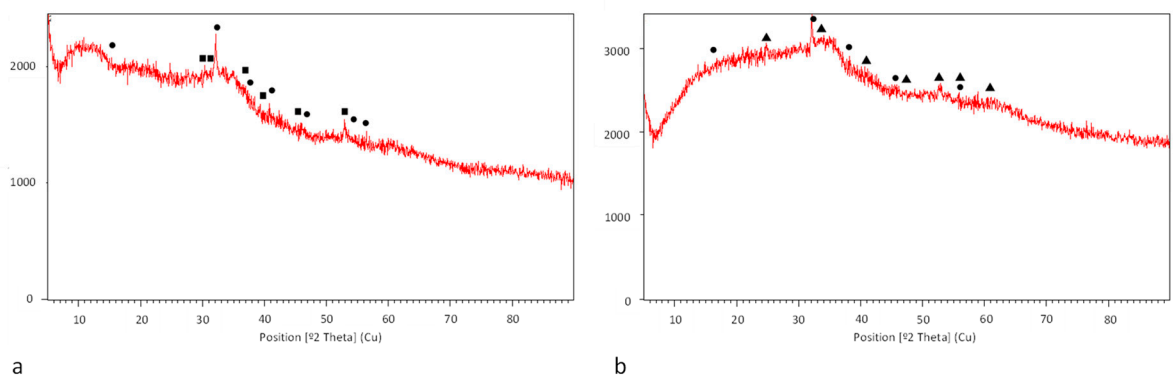

Figure 4. XRD patterns of iron precipitates produced by the natural consortium after the adsorption experiments with (**a**) As(III) and (**b**) As(V) (●, As_4O_6; ■, As_2O_3; ▲, As).

3.2. Arsenic Adsorption in Caracarani River Waters

The use of biogenic iron compounds as adsorbents in continuous systems is difficult due to their small size (Figure 5a). Iron precipitates were encapsulated in alginate beads to overcome the difficulties in the separation of micro/nano adsorbents from waters (Figure 5b).

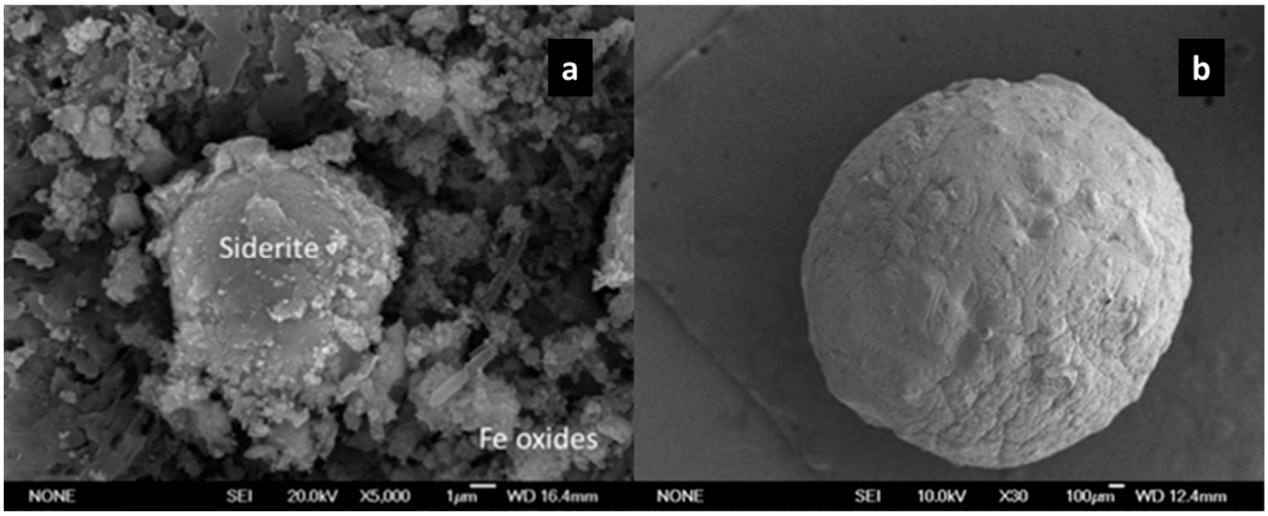

Figure 5. SEM images of (**a**) iron compounds produced by the microbial consortium and (**b**) alginate bead containing biogenic iron compounds.

Batch experiments for the treatment of Caracarani River waters were performed with the biogenic iron precipitates and with iron compound particles encapsulated in alginate beads at different pH values, as shown in Figure 6. Iron precipitates formed by the microbial consortium were able to remove arsenic ions from the polluted waters mainly at pH 2.24 (as received) while Zn^{2+} removal was very low because organic matter associated with the solid was involved in cation binding. At higher pH values, arsenic co-precipitates with the iron in solution and zinc is precipitated at pH 7 and 10.

Alginate beads encapsulating iron solids were able to adsorb not only the arsenic but also zinc ions. Alginate is a biocopolymer that contains alternating blocks of D-mannuronic and L-guluronic acids rich in carboxyl groups that play a major role in hazardous metal adsorption. The dissociation constant of carboxylic groups in the mannuronic acid is $pK_a = 3.38$ and in glucuronic acid is $pK_a = 3.65$ [32]. The carboxylic groups are bound to protons at pH values below the pK_a. In consequence, the access of metallic cations to these groups is limited due to repulsive forces. For this reason, zinc adsorption from polluted waters was very low at pH 2.24. At pH 4, carboxylates with negative charges are available and the uptake by alginate slightly increased. Probably, there is a competition between different cations present in the solution for the binding sites in the beads.

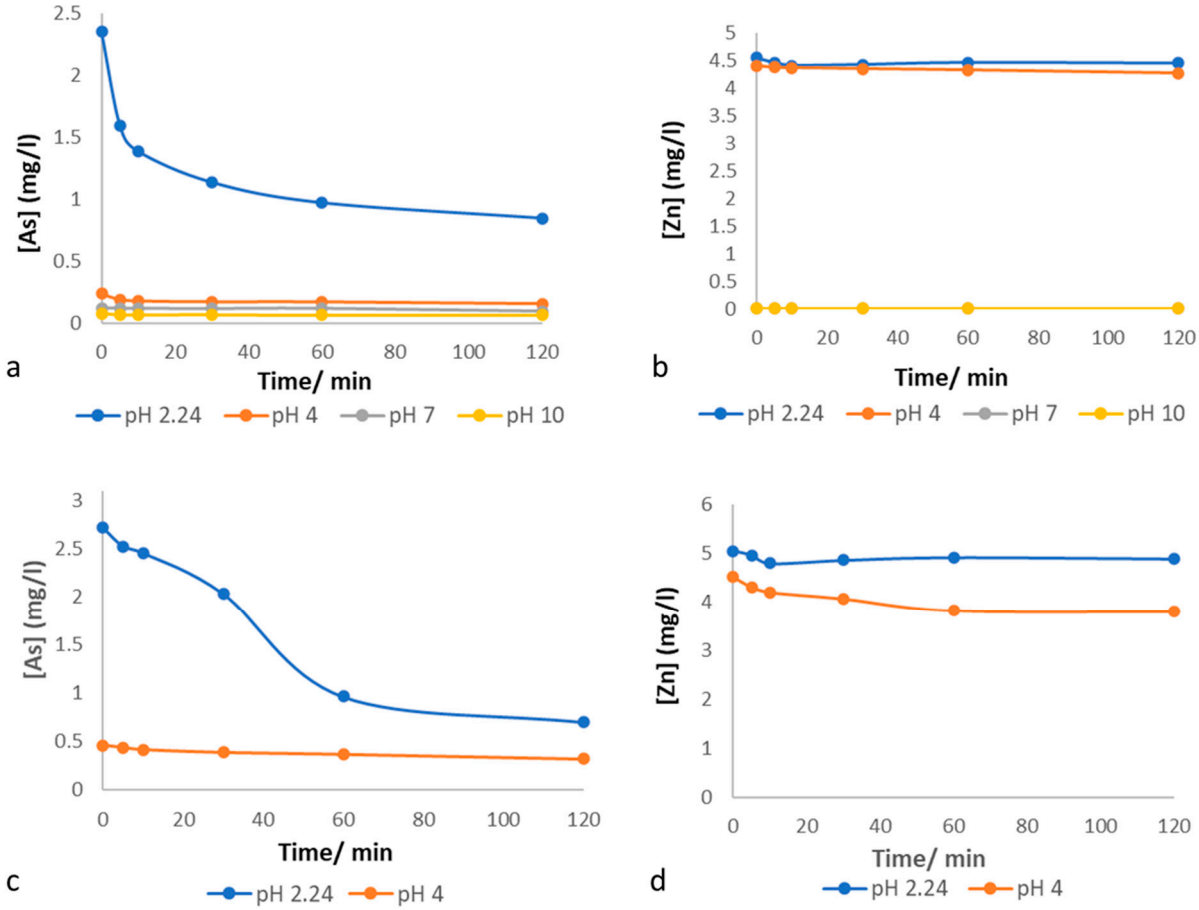

Figure 6. Effect of initial pH value on the pollutant adsorption from Caracarani River water using the biogenic iron precipitates (**a**) arsenic and (**b**) zinc; and using the iron precipitates/alginate beads (**c**) arsenic and (**d**) zinc. Adsorbent concentration: 1 g/L.

3.3. Continuous Adsorption Tests

The ability of biogenic iron compounds to adsorb the main metals present in the polluted water from Caracarani River under batch conditions has previously been demonstrated. Continuous experiments in column reactors are required to treat larger volumes. The experiments were carried out with real effluents from Caracarani River (Chile) at pH 2.24 and the adsorbent was the alginate beads immobilizing the biogenic iron precipitates.

3.3.1. Effect of Feed Flow Rate

Two columns with encapsulated biogenic iron compounds were tested at 2 and 1 mL/min and their column efficiency and contaminant uptake compared (Figure 7) (Table 3). Despite the increase in the flow rate enabling the decontamination of larger volumes in less time, higher flow rates led to a decrease in the saturation time of the columns, evidencing that the mass transfer zone became narrower.

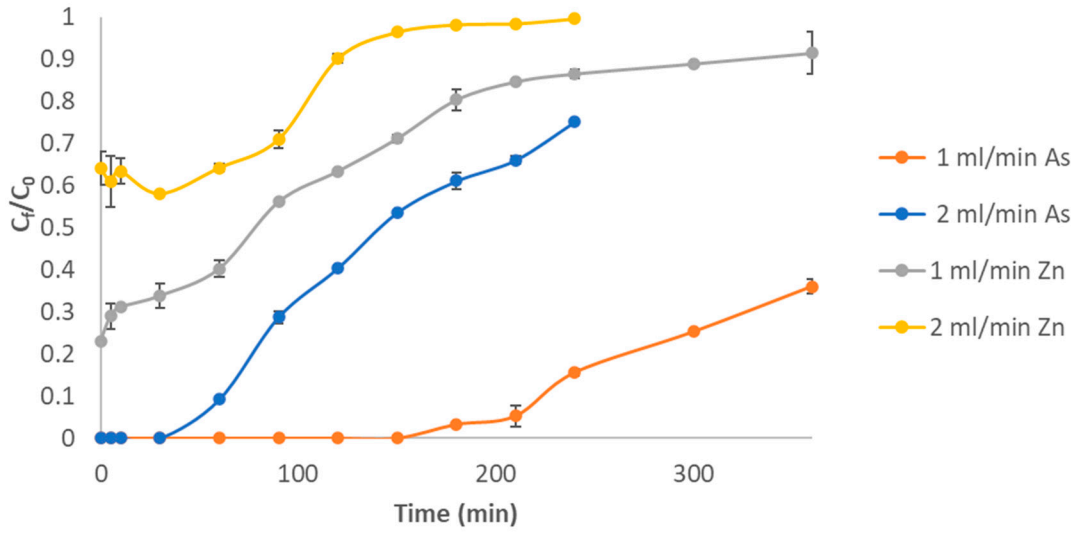

Figure 7. Arsenic and zinc sorption breakthrough curves of drop-fed columns with alginate beads containing biogenic iron compounds using different feed flow rates (3 cm of bed height (7.87 g of adsorbent)).

The saturation time increased from 150 min at a flow rate of 2 mL/min to 210 min at 1 mL/min, and the slope of the breakthrough curve decreased. The longer contact time between the solution and the beads is likely to have been the result of an increase in metal uptake.

3.3.2. Effect of Bed Height

The pollutant uptake in two columns with 3 cm (7.87 g of adsorbent) and 6 cm (13.35 g) of bed height and a flow rate of 1 mL/min are compared in Figure 8. The initial outlet concentration was influenced by bed height and was lower for the column containing a higher amount of adsorbent. An increase in the bed height led to longer saturation and service time of the reactor due to the higher quantity of beads. According to Table 3, the increase in the bed height led to higher adsorption capacities. At the lowest bed height there is not enough time for the ions to diffuse into the beads [33].

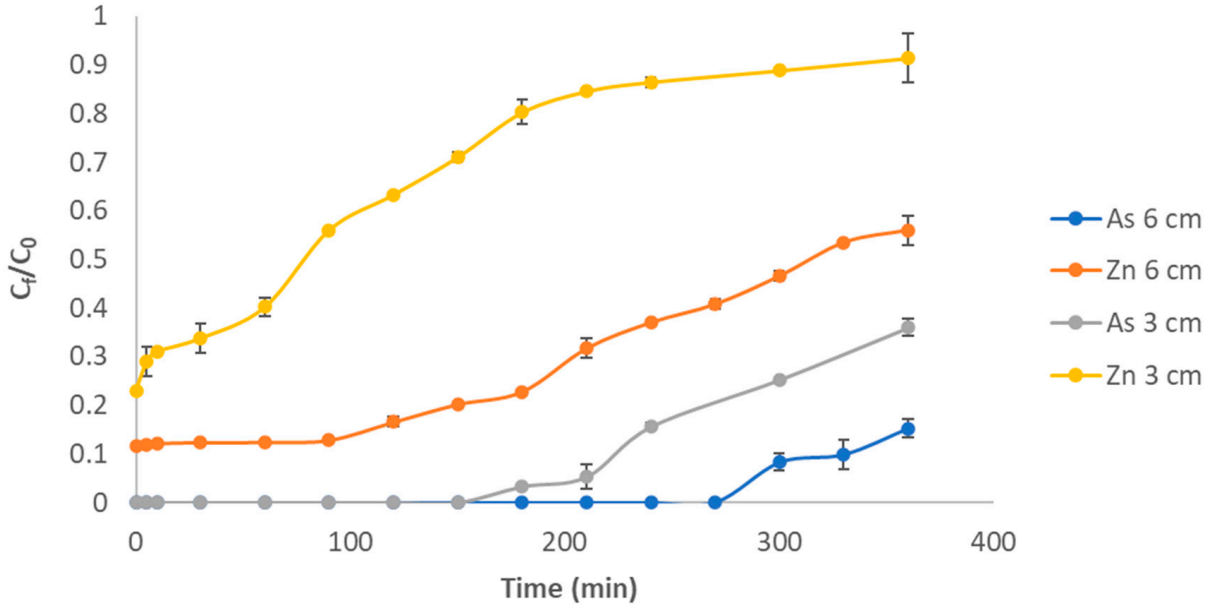

Figure 8. Arsenic and zinc sorption breakthrough curves of drop-fed columns with alginate beads containing biogenic iron compounds using different bed heights (1 mL/min flow rate).

3.3.3. Effect of Feeding System

The reverse-fed system was compared to drop-fed columns to increase the efficiency of the contact between the adsorbent and the polluted water avoiding preferential channels (Figure 9).

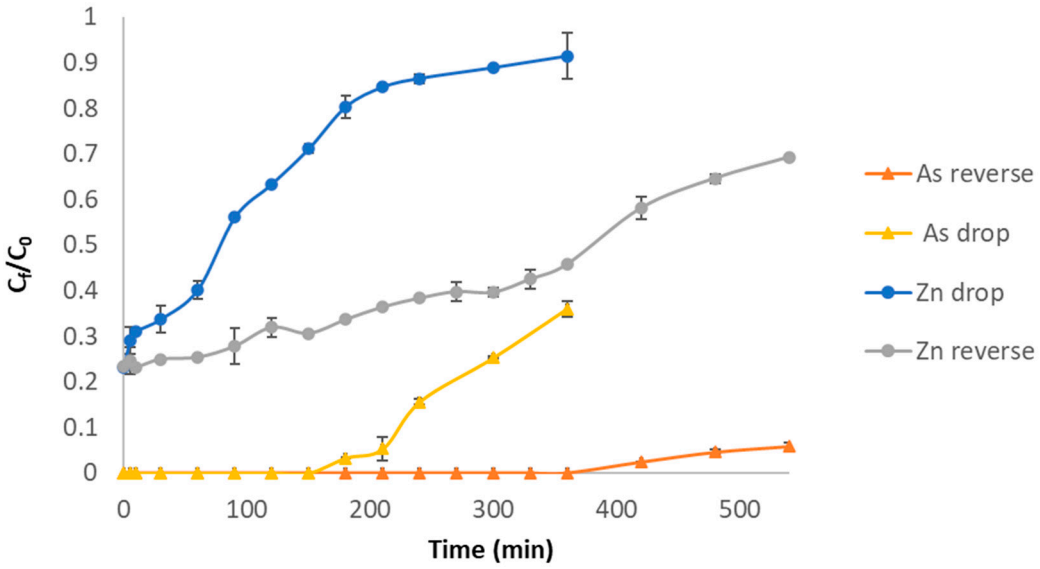

Figure 9. Arsenic and zinc adsorption breakthrough curves of columns with alginate beads containing biogenic iron compounds using drop and reverse feeding systems (3 cm of bed height (7.87 g of adsorbent) and 1 mL/min flow rate).

The effect of the feeding systems in the pollutant adsorption was remarkable. Saturation time and column efficiency notably increased in the reverse-fed system and arsenic concentration was not detected after 6 h of treatment. The reverse-fed column reached a higher metalloid adsorption in the same period (Table 3).

A significant difference between the drop-fed and the reverse-fed systems is the shape of the breakthrough curve. The curve was favorably modified in the reverse-fed column showing a steeper slope and a lag period that enhanced the service time of the reactor.

The scarcity of water resources has led to the use of high arsenic concentration waters in agriculture and other human activities. The contaminated water containing heavy metals can pollute the agricultural soil and crop plants with potential environmental and human health risks [34,35]. This study attempts to reduce the water pollution below the maximum legal limits for irrigation water (0.1 mg/L for arsenic and 2 mg/L in the case of zinc) [36]. The parameters of the continuous experiments are collected in Table 4 and the breakthrough point was the legal limit (although the column was not completely saturated), because it is the most relevant information for the implementation.

Continuous adsorption parameters were determined by studying the breakthrough curves of the columns. The amount of treated metal/metalloid (Me_{tr} (mmol)) and the retained pollutants by the column (Me_{ad} (mmol)) can be calculated as follows:

$$Me_{tr} = C_0 \quad (3)$$

$$Mead = A \cdot C_0 \cdot Q \quad (4)$$

where C_0 is the inlet metal/metalloid concentration (mmol/L); t is breakthrough time (h); Q is the flow rate (L/h) and A is the area under the breakthrough curve (h).

The adsorption yield (%Ad) and the adsorption capacity (q_c) of the columns can be calculated using the following expressions:

$$\%Ad = 100 \cdot Me_{ad}/Me_{tr} \quad (5)$$

$$q_c = Me_{ad}/m \quad (6)$$

where q_c is the adsorption capacity (mmol/g) and m is the amount of adsorbent in the column (g).

Table 4. Arsenic and zinc adsorption in columns charged with encapsulated biogenic iron under different experimental conditions.

Element	Feeding System	Adsorbent (g)	Flow Rate (mL/min)	Bed Height (cm)	Time (min)	Me_{tr} (mmol)	Me_{ad} (mmol)	% Ads	q_c (mmol/g)
As	Drop	7.87	1	3	90	2.77	2.77	100	0.35
Zn	Drop	7.87	1	3	90	6.40	3.92	61.2	0.50
As	Drop	13.35	1	6	270	8.07	8.06	99.9	0.51
Zn	Drop	13.35	1	6	270	21.12	16.61	78.6	1.06
As	Reverse	7.87	1	3	330	8.32	8.32	100	1.03
Zn	Reverse	7.87	1	3	330	26.47	18.36	69.4	2.33

The beads encapsulating the biogenic iron compounds were analyzed after the continuous experiments by X-ray diffraction. The diffractogram showed the presence of As^0 and $Zn_4(AsO_4)_2O$ (Figure 10). The adsorption and reduction of arsenate on iron precipitated at acidic pH values forming As^0 on the adsorbent surface was already evidenced. In addition, the coadsorption of Zn(II) and arsenate ions on the beads with iron precipitates could begin forming arsenate and zinc complexes on iron/alginate beads at lower concentrations, then the subsequent coprecipitation of Zn(II) and arsenate on the carboxylic groups of beads could lead to the formation of a surface precipitate $Zn_4(AsO_4)_2O$ at higher concentrations [37].

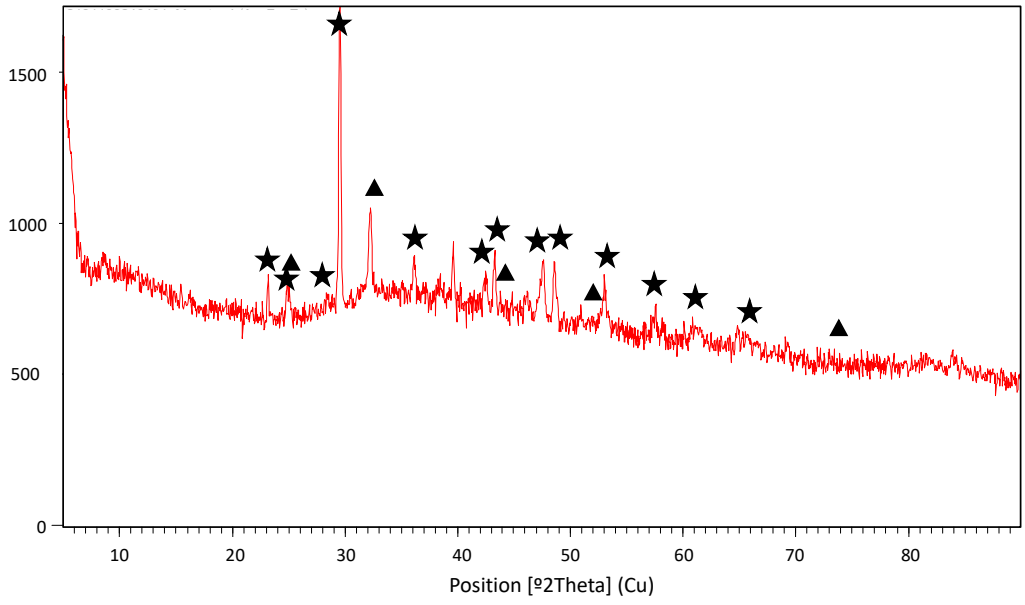

Figure 10. XRD patterns of alginate beads encapsulating biogenic iron precipitates after the continuous adsorption experiments with water from the river (▲, As^0; ★, $Zn_4(AsO_4)_2O$).

Alginate beads containing biogenic iron precipitates are cheap adsorbents for the removal of potentially toxic ions; nevertheless, the regeneration of the beads and their reuse in sorption–desorption cycles would be interesting from an economic point of view. Commonly, diluted acids are used as eluants with alginate; nevertheless, the adsorbent experiments show a significant loss of effectiveness after elution [38]. In addition, the

acidic pH could partially dissolve the iron particles resulting in the loss of the adsorbent mass. Sigdel et al. [39] reported that hydrous iron oxide-alginate beads could be effectively regenerated after arsenic adsorption using NaOH solutions (pH 10.5). A regeneration step with a mixture of $CaCl_2$ and dilute HCl at pH 6.5 was needed after the desorption process, and the removal efficiency decreased by almost 50%.

4. Conclusions

Secondary Fe(II)-bearing minerals precipitated during iron bioreduction are able to adsorb arsenic oxyanions due to the positive charge on the surface of the iron oxides. Arsenate adsorption capacities are higher than arsenite at their respective optimum pH values (pH 2 for As(V) and pH 10 for As(III)) due to arsenite existing mostly in neutral form, leading to a lack of attraction to adsorption sites. Furthermore, arsenate adsorption fitted to the Langmuir model (q_{max} = 0.64 mmol/g, K_L = 0.019 mmol/L) while arsenite fitted to the Freundlich model (K_F = 0.476 L/g, n = 2.13). As(III) and As(V) were strongly adsorbed onto the adsorbent through surface complexation and amorphous and/or nanocrystalline precipitates were formed.

Acidic waters from the Caracarani River (Chile) with high concentrations of arsenic and zinc were treated using the biogenic iron compounds. Iron precipitates were encapsulated in alginate beads for the continuous treatment of the polluted water. This material adsorbed arsenic in iron precipitates and carboxylate groups in alginate adsorbed zinc cations. The coadsorption of Zn(II) and arsenate ions on the beads with iron precipitates led to the formation of a surface precipitate ($Zn_4(AsO_4)_2O$).

The optimum conditions for arsenic and zinc adsorption with biogenic iron/alginate beads in continuous experiments were low feed flow rate (1 mL/min) and an up-flow system. The service time of the continuous reactors significantly decreased by increasing the flow rates and the formation of preferential flow channels. The reverse-fed system improved the operational efficiency of the columns avoiding the preferential channels through the fixed bed. The optimized conditions for the hazardous metal/metalloid adsorption using biogenic iron precipitates demonstrated that bionanotechnology can be applied in the treatment of real waters.

Author Contributions: Conceptualization, L.C. and J.Á.M.; funding acquisition, J.Á.M.; investigation, L.C., L.A.A.; methodology, L.A.A. and L.C.; project administration, J.Á.M.; resources, J.Á.M.; validation, R.Z. and A.V.; writing—review and editing, L.C., R.Z. and A.V. All authors have read and agreed to the published version of the manuscript.

Funding: This work was founded by the Spanish Ministry of Economy and Competitiveness (project MAT2014-59222R).

Institutional Review Board Statement: Not applicable.

Informed Consent Statement: Not applicable.

Data Availability Statement: Not applicable.

Conflicts of Interest: The authors declare no conflict of interest.

References

1. EPA (United States Environmental Protection Agency). Integrated Risk Information System (IRIS). 1991. Available online: https://www.epa.gov/iris (accessed on 31 August 2021).
2. Rasheed, H.; Kay, P.; Slack, R.; Gong, Y.Y. Arsenic species in wheat, raw and cooked rice: Exposure and associated health implications. *Sci. Total Environ.* **2018**, *634*, 366–373. [CrossRef]
3. WHO. *World Health Organization, Guidelines for Drinking Water Quality, Health Criteria and Other Supporting Information*; World Health Organization: Geneva, Switzerland, 2004.
4. Pal, P. Chapter 4—Arsenic removal by membrane filtration. In *Groundwater Arsenic Remediation*; Pal, P., Ed.; Butterworth-Heinemann: Oxford, UK, 2015; pp. 105–177.
5. Pal, P. Chapter 2—Chemical treatment methods in arsenic removal. In *Groundwater Arsenic Remediation*; Pal, P., Ed.; Butterworth-Heinemann: Oxford, UK, 2015; pp. 25–70.

6. Mondal, M.K.; Garg, R. A comprehensive review on removal of arsenic using activated carbon prepared from easily available waste materials. *Environ. Sci. Pollut. Res.* **2017**, *24*, 13295–13306. [CrossRef]
7. El-sayed, M.E.A. Nanoadsorbents for water and wastewater remediation. *Sci. Total Environ.* **2020**, *739*, 139903. [CrossRef]
8. Parkinson, G.S. Iron oxide surfaces. *Surf. Sci. Rep.* **2016**, *71*, 272–365.
9. Hennebel, T.; De Gusseme, B.; Boon, N.; Verstraete, W. Biogenic metals in advanced water treatment. *Trends Biotechnol.* **2009**, *27*, 90–98. [CrossRef] [PubMed]
10. Gadd, G.M. Metals, minerals and microbes: Geomicrobiology and bioremediation. *Microbiology* **2010**, *156*, 609–643. [CrossRef]
11. Park, D.; Yun, Y.-S.; Park, J.M. The past, present, and future trends of biosorption. *Biotechnol. Bioprocess Eng.* **2010**, *15*, 86–102. [CrossRef]
12. Amirnia, S.; Ray, M.B.; Margaritis, A. Heavy metals removal from aqueous solutions using *Saccharomyces cerevisiae* in a novel continuous bioreactor–biosorption system. *Chem. Eng. J.* **2015**, *264*, 863–872. [CrossRef]
13. Castro, L.; Rocha, F.; Muñoz, J.Á.; González, F.; Blázquez, M.L. Batch and continuous chromate and zinc sorption from electroplating effluents using biogenic iron precipitates. *Minerals* **2021**, *11*, 349. [CrossRef]
14. Zhou, J.-X.; Zhou, Y.-J.; Zhang, J.; Dong, Y.; Liu, F.-W.; Wu, Z.-H.; Bi, W.-L.; Qin, J.-M. Effect of pH regulation on the formation of biogenic schwertmannite driven by *Acidithiobacillus ferrooxidans* and its arsenic removal ability. *Environ. Technol.* **2021**. [CrossRef]
15. Saunders, J.A.; Lee, M.-K.; Dhakal, P.; Ghandehari, S.S.; Wilson, T.; Billor, M.Z.; Uddin, A. Bioremediation of arsenic-contaminated groundwater by sequestration of arsenic in biogenic pyrite. *Appl. Geochem.* **2018**, *96*, 233–243. [CrossRef]
16. Liu, J.; Zhou, L.; Dong, F.; Hudson-Edwards, K.A. Enhancing As(V) adsorption and passivation using biologically formed nano-sized FeS coatings on limestone: Implications for acid mine drainage treatment and neutralization. *Chemosphere* **2017**, *168*, 529–538. [CrossRef] [PubMed]
17. Lee, C.; Jung, J.; Pawar, R.R.; Kim, M.; Lalhmunsiama; Lee, S.-M. Arsenate and phosphate removal from water using Fe-sericite composite beads in batch and fixed-bed systems. *J. Ind. Eng. Chem.* **2017**, *47*, 375–383. [CrossRef]
18. Castro, L.; Blázquez, M.L.; González, F.; Muñoz, J.A.; Ballester, A. Heavy metal adsorption using biogenic iron compounds. *Hydrometallurgy* **2018**, *179*, 44–51. [CrossRef]
19. Guerra, P.; Simonson, K.; González, C.; Gironás, J.; Escauriaza, C.; Pizarro, G.; Bonilla, C.; Pasten, P. Daily freeze–thaw cycles affect the transport of metals in streams affected by acid drainage. *Water* **2016**, *8*, 74. [CrossRef]
20. Guerra, P.; Gonzalez, C.; Escauriaza, C.; Pizarro, G.; Pasten, P. Incomplete mixing in the fate and transport of arsenic at a river affected by acid drainage. *Water Air Soil Pollut.* **2016**, *227*, 73. [CrossRef]
21. Stanić, T.; Daković, A.; Živanović, A.; Tomašević-Čanović, M.; Dondur, V.; Milićević, S. Adsorption of arsenic (V) by iron (III)-modified natural zeolitic tuff. *Environ. Chem. Lett.* **2009**, *7*, 161–166. [CrossRef]
22. Das, T.K.; Sakthivel, T.S.; Jeyaranjan, A.; Seal, S.; Bezbaruah, A.N. Ultra-high arsenic adsorption by graphene oxide iron nanohybrid: Removal mechanisms and potential applications. *Chemosphere* **2020**, *253*, 126702. [CrossRef]
23. Pan, H.; Hou, H.; Chen, J.; Li, H.; Wang, L. Adsorption of arsenic on iron modified attapulgite (Fe/ATP): Surface complexation model and DFT studies. *Adsorption* **2018**, *24*, 459–469. [CrossRef]
24. Chen, B.; Zhu, Z.; Liu, S.; Hong, J.; Ma, J.; Qiu, Y.; Chen, J. Facile hydrothermal synthesis of nanostructured hollow iron–cerium alkoxides and their superior arsenic adsorption performance. *ACS Appl. Mater. Interfaces* **2014**, *6*, 14016–14025. [CrossRef]
25. Vieira, B.R.C.; Pintor, A.M.A.; Boaventura, R.A.R.; Botelho, C.M.S.; Santos, S.C.R. Arsenic removal from water using iron-coated seaweeds. *J. Environ. Manag.* **2017**, *192*, 224–233. [CrossRef]
26. Nguyen, T.V.; Vigneswaran, S.; Ngo, H.H.; Kandasamy, J. Arsenic removal by iron oxide coated sponge: Experimental performance and mathematical models. *J. Hazard. Mater.* **2010**, *182*, 723–729. [CrossRef] [PubMed]
27. Zeng, H.; Zhai, L.; Qiao, T.; Zhang, J.; Li, D. Removal of As(V) by a core-shell magnetic nanoparticles synthesized with iron-containing water treatment residuals. *Colloids Surf. A Physicochem. Eng. Asp.* **2021**, *627*, 127074. [CrossRef]
28. Wang, Y.; Morin, G.; Ona-Nguema, G.; Brown, G.E. Arsenic(III) and arsenic(V) speciation during transformation of lepidocrocite to magnetite. *Environ. Sci. Technol.* **2014**, *48*, 14282–14290. [CrossRef] [PubMed]
29. Wang, Y.; Morin, G.; Ona-Nguema, G.; Juillot, F.; Calas, G.; Brown, G.E. Distinctive arsenic(V) trapping modes by magnetite nanoparticles induced by different sorption processes. *Environ. Sci. Technol.* **2011**, *45*, 7258–7266. [CrossRef] [PubMed]
30. Morin, G.; Wang, Y.; Ona-Nguema, G.; Juillot, F.; Calas, G.; Menguy, N.; Aubry, E.; Bargar, J.R.; Brown, G.E. EXAFS and HRTEM evidence for As(III)-containing surface precipitates on nanocrystalline magnetite: Implications for As sequestration. *Langmuir* **2009**, *25*, 9119–9128. [CrossRef]
31. Perez, J.P.H.; Tobler, D.J.; Thomas, A.N.; Freeman, H.M.; Dideriksen, K.; Radnik, J.; Benning, L.G. Adsorption and reduction of arsenate during the Fe^{2+}-induced transformation of ferrihydrite. *ACS EarthSpace Chem.* **2019**, *3*, 884–894. [CrossRef]
32. Rehm, B.H.A. *Alginates: Biology and Applications*; Springer: Berlin/Heidelberg, Germany, 2009.
33. Mondal, M.K. Removal of Pb(II) ions from aqueous solution using activated tea waste: Adsorption on a fixed-bed column. *J. Environ. Manag.* **2009**, *90*, 3266–3271. [CrossRef]
34. He, L.; Hu, W.; Wang, X.; Liu, Y.; Jiang, Y.; Meng, Y.; Xiao, Q.; Guo, X.; Zhou, Y.; Bi, Y.; et al. Analysis of heavy metal contamination of agricultural soils and related effect on population health-a case study for east river basin in China. *Int. J. Environ. Res. Public Health* **2020**, *17*, 1996. [CrossRef]
35. Bhatia, A.; Singh, S.; Kumar, A. Heavy metal contamination of soil, irrigation water and vegetables in peri-urban agricultural areas and markets of Delhi. *Water Environ. Res.* **2015**, *87*, 2027–2034. [CrossRef]

36. Ayers, R.S.; Westcot, D.W. *Water Quality for Agriculture*; FAO irrigation and drainage paper; Food and Agriculture Organization of the United Nations: Rome, Italy, 1994; Volume 29.
37. Carabante, I.; Grahn, M.; Holmgren, A.; Kumpiene, J.; Hedlund, J. Influence of Zn(II) on the adsorption of arsenate onto ferrihydrite. *Environ. Sci. Technol.* **2012**, *46*, 13152–13159. [CrossRef] [PubMed]
38. Castro, L.; Blázquez, M.L.; González, F.; Muñoz, J.A.; Ballester, A. Biosorption of Zn(II) from industrial effluents using sugar beet pulp and *F. vesiculosus*: From laboratory tests to a pilot approach. *Sci. Total Environ.* **2017**, *598*, 856–866. [CrossRef] [PubMed]
39. Sigdel, A.; Lim, J.; Park, J.; Kwak, H.; Min, S.; Kim, K.; Lee, H.; Nahm, C.H.; Park, P.-K. Immobilization of hydrous iron oxides in porous alginate beads for arsenic removal from water. *Environ. Sci. Water Res. Technol.* **2018**, *4*, 1114–1123. [CrossRef]